

Research Article

Iterative Learning Control for Nonlinear Weighing and Feeding Process

Jianqi An ^{1,2,3}, Fayang You,^{1,2} Min Wu,^{1,2} and Jinhua She^{1,2,3}

¹School of Automation, China University of Geosciences, Wuhan 430074, China

²Hubei Key Laboratory of Advanced Control and Intelligent Automation for Complex Systems, Wuhan 430074, China

³School of Engineering, Tokyo University of Technology, Tokyo 192-0982, Japan

Correspondence should be addressed to Jianqi An; anjianqi@cug.edu.cn

Received 7 September 2018; Accepted 25 November 2018; Published 20 December 2018

Academic Editor: AITOU CHE Abdelouhab

Copyright © 2018 Jianqi An et al. This is an open access article distributed under the Creative Commons Attribution License, which permits unrestricted use, distribution, and reproduction in any medium, provided the original work is properly cited.

Due to the nonlinear dynamics in weighing and feeding process, it is difficult to achieve high accuracy with conventional control methods. This paper uses a piecewise linearization method for the nonlinear problem and discusses the application of iterative learning control in weighing and feeding process. First, the nonlinear problem and the repeatability are discussed based on dynamic analysis of weighing and feeding process. Next, a linear state space model is established with a piecewise linearization method. Then, an iterative learning controller is presented by utilizing repetitive characteristics, and the controller parameters are obtained by using a multi-objective optimization method. Finally, simulation results show that the presented control method improves the control performances and the accuracy of feeding.

1. Introduction

A weighing and feeding process is a process in which a certain material is weighted and added to a reaction vessel through an actuator, which repeats many times to get more products. It is widely used in modern industries, such as metallurgical industry, pharmaceutical industry, and food processing industry [1]. Vibratory feeders are the main actuators in weighing and feeding processes, which use vibration and gravity to feed material to a weighing hopper. The weight of the material in the weighing hopper is one of the most important control objectives in a weighing and feeding process. However, it is difficult to achieve high accuracy of the weight because of the existence of a nonlinear process of the vibratory feeder [2].

In the past few years, some good methods were researched to establish accurate mathematical models for vibratory feeders. For example, a model of a resonant linear electromagnetic vibratory feeder was established based on the kinetic and potential energies, the dissipative function of the mechanical system, and Lagrangian formulation [3]. Czubak [4] considered the vibratory feeder as a single degree of

freedom system (SDOF). The relations between the structural elements of the mode and the vibratory feeder were analyzed based SDOF [5]. Furthermore, Chandravanshi [6, 7] analyzed the dynamic characteristics of vibratory feeders and examined experimentally the vibration behavior of the particles on the conveying surface. The purposes of these researches are to dynamically analyze the vibratory feeders and the vibration behavior of the particles. These researches reveal the nonlinear relationship between the feed rate and the motor speed (vibratory motors rotate to generate vibration to make the vibratory feeder work). It is obvious that vibratory feeders are nonlinear devices in weighing and feeding processes.

Regarding the control and modeling of weighing and feeding processes, many results were published for one feeding batch, which considered the vibrating feeder as a linear device. For instance, a generalized-predictive-control (GPC)-based PID controller was presented for a linear weighing and feeding process, which considered the relationship between the feed rate and motor speed as a linear model [8]. This method derived PID parameters based on GPC and considered a ramp-type signal as the reference signal. The method presented in [8] was improved in [9], in which the

TABLE I: Some notations used in this paper.

Symbol	Definition
t, k	The time and batch index, respectively
α, β	The time period in a batch and the total number of batches, respectively
R	The set of real number
$I, \mathbf{0}$	The identity matrix and the zero matrix with appropriate dimensions, respectively
f, U	The output frequency and input voltage of the inverter, respectively
ω	The motor speed
v	The feeding rate
w	The weight of the material in the weighing hopper

estimated plant parameters are updated when the prediction error increases. A feedback controller was used in the control of an electromagnetic vibratory feeder, in which the vibratory feeder is considered as a linear device [10]. And an amplitude-frequency control method of the vibratory feeder is presented by using a current-controlled power converter [11]. The previous researches on the weighing and feeding processes achieved good results. However, the achieved control accuracy can be further improved by considering the nonlinear characters and the repetitive nature of weighing and feeding processes.

In summary, previous researches on modeling of vibratory feeders had proven that vibratory feeders are nonlinear devices. However, previous researches on the control and modeling of weighing and feeding processes did not consider the nonlinear characters of the weighing and feeding process. In our previous paper [12], the repetitive nature of a weighing and feeding process was considered, and then the feeding accuracy was improved to some extent. However, this performance improvement is limited because the paper did not consider the nonlinear characters of vibratory feeders.

Many good methods were presented to solve nonlinear problems, such as the fixed point index theory in cones which proved the existence of positive solutions of nonlinear boundary value problem [13, 14], the method of upper and lower solutions and different monotone iterative techniques which analyzed a nonlinear third-order differential equation [15], a weighted norm method which analyzed nonlinear Schrodinger equations [16], and using neural networks to approximate the nonlinear function [17, 18]. These researches provide good references for the nonlinear problem of weighing and feeding processes. Iterative learning control (ILC) [19] can improve the control performance with the increasing number of the batch by taking full advantage of the history control information to correct control input. With the effectivity of solving the problems with repetitive characteristics, ILC is widely used in the batch processes [20, 21] and repetitive processes [22, 23].

For the repeatability and the nonlinear problem of weighing and feeding processes, this paper presents an ILC and a piecewise linearization method. The rest of this paper is organized as follows: Section 2 analyzes the dynamic characteristics and the nonlinear problem of the process and then establishes an approximate linear model. Section 3 gives a 2D ILC system based on an improved state space model and a

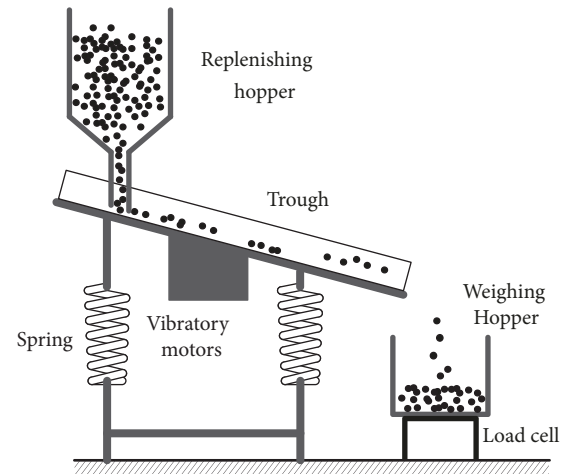


FIGURE 1: Weighing and feeding process.

controller parametrization method by using a multi-objective optimization method. Section 4 gives the simulation results to illustrate the effectiveness of the proposed method. Finally, Section 5 draws a conclusion.

Some notations used in this paper are described in Table 1.

2. Analysis and Modeling of Weighing and Feeding Process

This section presents the structure of a weighing and feeding process, analyzes the dynamic characteristic of the weighing and feeding process, discusses its nonlinear problem, and presents an approximate linear model by using a piecewise linearization method.

2.1. Weighing and Feeding Process. The schematic diagram of a weighing and feeding process is shown in Figure 1. The vibratory feeder is the main device, which consists of springs for damping, vibration motors for oscillating, and a trough for conveying material. The vibration motors are fixed under the bottom of the trough, which generates an exciting force by driving a rotating unbalanced mass. The trough is inclined at an angle which performs sinusoidal vibration caused by the exciting force. When the trough vibrates due to the exciting force, materials are shaken into the weighing hopper by

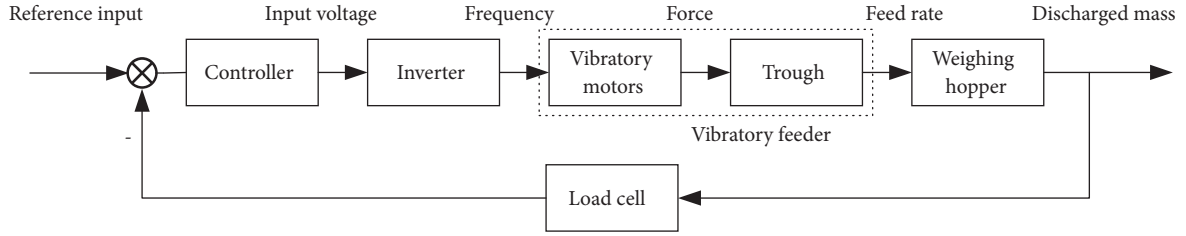


FIGURE 2: Weighing and feeding process control system.

the vibrating trough. Weighing hopper measures materials weight by a load cell. The feed rate of the material is adjusted by changing the exciting force and the vibration frequency. In addition, the replenishing hopper replenishes the loss material on the trough. The spring is installed between the trough and the support unit to reduce damage to the support unit caused by the vibration motors.

The block diagram of weighing and feeding process control system is shown in Figure 2, which consists of a controller, an inverter, a vibratory feeder, a weighing hopper, and a load cell. The controller adjusts the speed of the motor by changing the input voltage of the inverter. When the weight of material reaches the set value, the vibratory feeder stops working and prepares for the next batch. In order to get more products, the feeding process like that repeats many times.

The dynamic characteristics of the inverter are approximated as an amplifier [8], which is expressed as

$$f = K_i U, \quad (1)$$

where K_i is the gain of the inverter. f and U denote the output frequency and input voltage of the inverter, respectively.

The trough of the vibratory feeder vibrates under the drive of double rotating unbalances which produces a periodic force excitation in a definite direction. The electrical model of the motor can be written as a first-order system

$$\dot{\omega} + \frac{1}{T}\omega = \frac{K_m}{T}f, \quad (2)$$

where K_m is the gain and T is assumed to be the time constant of the motor.

The exciting forces, F_1 and F_2 , are induced by a single rotating unbalance mass (see Figure 3), m , respectively. The values of F_1 and F_2 are both given as

$$F_0 = mE\omega^2, \quad (3)$$

where E is the eccentricity of the unbalance.

Decomposition of excitation force into horizontal and vertical directions

$$F_x = F_0 \cos \omega t + F_0 \cos(\pi - \omega t) = 0, \quad (4)$$

$$F_y = F_0 \sin \omega t + F_0 \sin(\pi - \omega t) = 2F_0 \sin \omega t. \quad (5)$$

The mechanical model of the vibratory feeder is assumed as an SDOF which consists of a mass, M , spring with stiffness

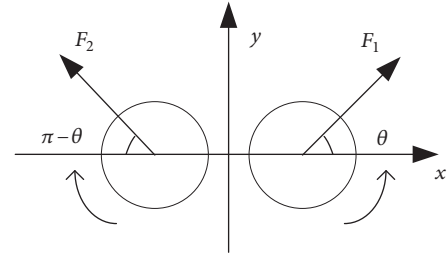


FIGURE 3: The exciting force.

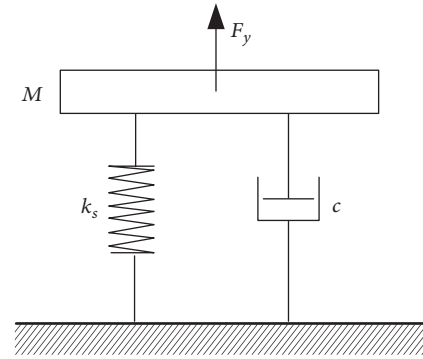


FIGURE 4: The mechanical model of the vibratory feeder.

coefficient, k_s , and damping with damping coefficient, c , [5] as shown in Figure 4.

The equation of the vibration is expressed as

$$M \frac{d^2 Y}{dt^2} + c \frac{dY}{dt} + k_s Y = F_y, \quad (6)$$

where M is the equivalent weight which consists of the weight of the vibratory motor, the trough, and the materials in the trough. Y denotes the displacement from the balance position in vertical directions. The damping is the consumption of vibratory energy as heat and sound. k_s is the equivalent stiffness of springs. The exciting force in vertical directions changes sinusoidally. By analyzing (6) through vibration theory, the maximum amplitude, Y_{\max} , of the vibratory trough is written as

$$Y_{\max} = \frac{2F_0}{\sqrt{(k_s - \omega^2 M)^2 + (\omega c)^2}}. \quad (7)$$

The moving distance of the material in the trough is related to the vibration amplitude in one vibration. During a certain period of time, all the materials in the trough move multiple times to form an average feed rate. The average feed rate, v , and the maximum amplitude of vibration are approximately proportion

$$v = K \frac{\omega}{2\pi} Y_{\max}, \quad (8)$$

where K is the structure coefficient, which depends on the width of the trough and the angle of inclination of the trough.

Vibratory feeder adds material to the hopper, which can be approximated as an integrator

$$w = \int v dt, \quad (9)$$

where w denotes the weight of the material in the weighing hopper.

2.2. Piecewise Linearization Method. By substituting (7) into (8), the relationship between the feeding rate and the motor speed is written as

$$v = \frac{K m E \omega^3}{\pi \sqrt{(k_s - \omega^2 M)^2 + (\omega c)^2}}. \quad (10)$$

It is obvious that the feed rate increases first and then decreases when the motor speed increases through mathematic analysis of the relationship between v and ω . And when the vibration frequency of the vibratory motor is equal to the natural frequency, ω_n , the vibrating feeder reaches the maximum feeding rate. At this time, the motor speed ω_n is

$$\omega_n = \sqrt{\frac{k_s}{M}}. \quad (11)$$

Through the analysis of the relationship between the feeding rate and the motor speed, the feeding rate is decreasing when the motor speed is increasing ($\omega > \omega_n$). It should be avoided to work in this state because increasing the speed of the motor reduces the feeding speed, which is an inefficient production way.

Based on the considerations above, the motor of vibratory feeder should work in motor speed range $0 < \omega < \omega_n$. Then, the nonlinear relationship between motor speed and feeding rate is piecewise linearized into proportional relation

$$v = \begin{cases} a_1 \omega + b_1, & 0 \leq \omega < \omega_1 \\ a_2 \omega + b_2, & \omega_1 \leq \omega < \omega_2, \\ a_3 \omega + b_3, & \omega_2 \leq \omega < \omega_3 \end{cases} \quad (12)$$

which can be written as

$$v = a_i \omega + b_i, \quad \omega \in \Omega_i, \quad 1 \leq i \leq 3. \quad (13)$$

The nonlinear character and the piecewise linearization result are shown in Figure 5. In this paper, the motor

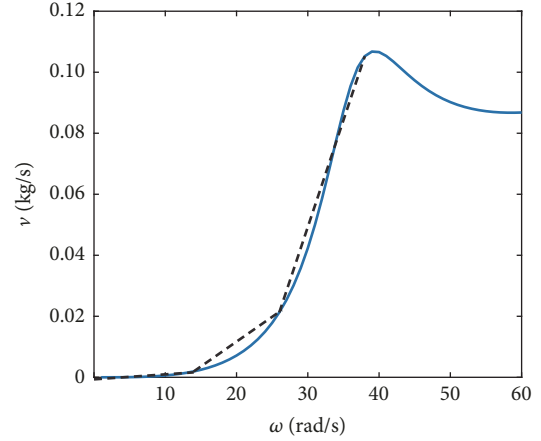


FIGURE 5: The relationship between feeding rate and motor speed.

speed range is divided equally into three intervals. Then the parameters of (13) are obtained by the corresponding motor speed and feeding rate. The accuracy of the piecewise linearized model significantly depends on the number of the intervals and more intervals can increase the accuracy of the piecewise linearized model.

Use the following coordinate transformation

$$\bar{v} = \begin{bmatrix} v \\ 0 \end{bmatrix}, \quad (14)$$

$$\bar{\omega} = \begin{bmatrix} \omega \\ 1 \end{bmatrix}. \quad (15)$$

Then the nonlinear relationship between the feeding rate and the motor speed transforms into an approximate linear model

$$\bar{v} = \begin{bmatrix} a_i & b_i \\ 0 & 0 \end{bmatrix} [\bar{\omega}], \quad \bar{\omega} \in \bar{\Omega}_i, \quad 1 \leq i \leq 3. \quad (16)$$

2.3. The State Space Model of the Weighing and Feeding Process. According to the previous analysis, the relationship between motor speed and the input voltage is obtained from (1) and (2), the relationship between motor speed and the feeding rate is obtained from (16), and the relationship between the feeding rate and the weight of the material in the weighing hopper is obtained from (9). They are used as parts of (17) and (18). Then the model of the control object is described as

$$\dot{x} = \begin{bmatrix} \dot{\omega} \\ 0 \\ \dot{w} \end{bmatrix} = \begin{bmatrix} -\frac{1}{T} & 0 & 0 \\ 0 & 0 & 0 \\ a_i & b_i & 0 \end{bmatrix} \begin{bmatrix} \omega \\ 1 \\ w \end{bmatrix} + \begin{bmatrix} \frac{K_m K_i}{T} \\ 0 \\ 0 \end{bmatrix} u, \quad (17)$$

$$1 \leq i \leq 3,$$

$$y = [0 \ 0 \ 1] x. \quad (18)$$

3. Iterative Learning Control System

This section discusses the batch characteristic of weighing and feeding process and gives the structure of iterative learning controller based on an improved state space model. Then the controller parameters are found through a multi-objective optimization method.

3.1. 2D System Representation. A discrete state space equation which is obtained by using the zero-order hold to discrete (17) and (18) over $1 \leq t \leq \alpha, k \geq 1$ is

$$x_k(t+1) = A_i x_k(t) + B_i u_k(t), \quad 1 \leq i \leq 3, \quad (19)$$

$$y_k(t) = C x_k(t), \quad (20)$$

where $u_k(t) \in R$ is the control input, $y_k(t) \in R$ is the output, $x_k(t) \in R^2$ is the state vector, including the motor speed ω , and the discharged mass w at time t in k th batch.

The discrete dynamic model in the k th batch is described as above. However, this process will be repeated many times to get more products in practice. Based on the above considerations, define $x(t, k)$, and $y(t, k)$ as the state and output of the process at time t in k th batch. The following discrete model can be established from (19) and (20) to describe the relationship between batches:

$$x(t+1, k) = A_i x(t, k) + B_i u(t, k), \quad 1 \leq i \leq 3, \quad (21)$$

$$y(t, k) = C x(t, k). \quad (22)$$

Let $y_{ref}(t)$ be a vector-valued reference representing desired output behavior. Then the error in the k th batch is

$$e(t, k) \triangleq y_{ref}(t) - y(t, k). \quad (23)$$

In ILC, a general form of the control law is

$$\Sigma_{ilc} : \begin{cases} u(t, k) = u(t, k-1) + u_e(t, k) \\ u(t, 0) = 0, \end{cases} \quad (24)$$

where $u(t, k)$ is constructed from the control in previous batch and a correction term $u_e(t, k)$ from the history control information and $u(t, 0)$ denotes the initial control. $u_e(t, k)$ is the updating law to be determined.

Define $f_e(t, k+1)$ as the difference of f between two consecutive batches

$$f_e(t, k+1) \triangleq f(t, k+1) - f(t, k), \quad (25)$$

where f may be state x or output y and thus is in accordance with the ILC updating law shown in (24).

The tracking error integral $\sum e(t, k+1)$ is an additional state variable in ILC design, which is defined as

$$\sum e(t, k+1) \triangleq \sum_{i=0}^t e(i, k+1). \quad (26)$$

It follows from (21), (22) and (25) that

$$x_e(t+1, k+1) = A_i x_e(t, k+1) + B_i u_e(t, k+1), \quad (27)$$

$$1 \leq i \leq 3.$$

Equation (23) can be written as

$$\begin{aligned} e(t+1, k+1) &= y_{ref}(t+1) - y(t+1, k+1) \\ &\quad + y(t+1, k) - y(t+1, k) \\ &= e(t+1, k) - y_e(t+1, k+1). \end{aligned} \quad (28)$$

It follows from (21), (22), (25), and (27) that

$$y_e(t+1, k+1) = C A_i x_e(t, k+1) + C B_i u_e(t, k+1), \quad (29)$$

$$1 \leq i \leq 3.$$

According to (29), (28) can be written as

$$\begin{aligned} e(t+1, k+1) &= e(t+1, k) - C A_i x_e(t, k+1) \\ &\quad - C B_i u_e(t, k+1). \end{aligned} \quad (30)$$

It follows from (26) and (30) that

$$\begin{aligned} \sum e(t+1, k+1) &= \sum e(t, k+1) + e(t+1, k) \\ &\quad - C A_i x_e(t, k+1) \\ &\quad - C B_i u_e(t, k+1), \quad 1 \leq i \leq 3. \end{aligned} \quad (31)$$

Introduce a new state variable as

$$\hat{x}(t+1, k+1) = \begin{bmatrix} x_e(t+1, k+1) \\ e(t+1, k+1) \\ \sum e(t+1, k+1) \end{bmatrix}. \quad (32)$$

Then the corresponding state space model is derived as

$$\begin{aligned} \hat{x}(t+1, k+1) &= A_{i,1} \hat{x}(t, k+1) + A_{i,2} \hat{x}(t+1, k) \\ &\quad + \hat{B}_i u_e(t, k+1), \quad 1 \leq i \leq 3, \end{aligned} \quad (33)$$

where

$$A_{i,1} = \begin{bmatrix} A_i & \mathbf{0} & \mathbf{0} \\ -C A_i & \mathbf{0} & \mathbf{0} \\ -C A_i & \mathbf{0} & \mathbf{I} \end{bmatrix}, \quad (34)$$

$$A_{i,2} = \begin{bmatrix} \mathbf{0} & \mathbf{0} & \mathbf{0} \\ \mathbf{0} & \mathbf{I} & \mathbf{0} \\ \mathbf{0} & \mathbf{I} & \mathbf{0} \end{bmatrix}, \quad (35)$$

$$\hat{B}_i = \begin{bmatrix} B_i \\ -C B_i \\ -C B_i \end{bmatrix}. \quad (36)$$

3.2. Controller Design. Design an updating law as

$$u_e(t, k+1) = K_{i,1} \hat{x}(t, k+1) + K_{i,2} \hat{x}(t+1, k), \quad (37)$$

$$1 \leq i \leq 3,$$

where

$$K_{i,1} = [K_{i,11} \quad K_{i,12} \quad K_{i,13}], \quad (38)$$

$$K_{i,2} = [K_{i,21} \quad K_{i,22} \quad K_{i,23}]. \quad (39)$$

Then an improved 2D system of (21) and (22) is given by

$$\begin{aligned} \hat{x}(t+1, k+1) &= \widehat{A}_{i,1} \hat{x}(t, k+1) + \widehat{A}_{i,2} \hat{x}(t+1, k), \\ &1 \leq i \leq 3, \end{aligned} \quad (40)$$

where

$$\widehat{A}_{i,1} = \begin{bmatrix} A_i + B_i K_{i,11} & B_i K_{i,12} & B_i K_{i,13} \\ -CA_i - CB_i K_{i,11} & -CB_i K_{i,12} & -CB_i K_{i,13} \\ -CA_i - CB_i K_{i,11} & -CB_i K_{i,12} & I - CB_i K_{i,13} \end{bmatrix}, \quad (41)$$

$$\widehat{A}_{i,2} = \begin{bmatrix} B_i K_{i,21} & B_i K_{i,22} & B_i K_{i,23} \\ -CB_i K_{i,21} & I - CB_i K_{i,22} & -CB_i K_{i,23} \\ -CB_i K_{i,21} & I - CB_i K_{i,22} & -CB_i K_{i,23} \end{bmatrix}. \quad (42)$$

More states information of (21) and (22) is considered, and the control law (37) contains control information of the current and historical batches. The appropriate controller parameters, $K_{i,1}$, $K_{i,2}$, will give the system a better control performance.

3.3. Stability Analysis

Theorem 1. *The closed-loop 2D system in (40) is asymptotically stable and if symmetric positive matrices $P > Q$ exist, the following linear matrix inequality holds*

$$\psi_i = \begin{bmatrix} -P & PA_{i,1} + Y_1 & PA_{i,2} + Y_2 \\ * & -Q & \mathbf{0} \\ * & * & -P + Q \end{bmatrix} < 0, \quad (43)$$

where

$$Y_1 = P\widehat{B}_i K_{i,1}, \quad (44)$$

$$Y_2 = P\widehat{B}_i K_{i,2}. \quad (45)$$

And the controller parameters $K_{i,1}$, $K_{i,2}$ can be solved as

$$K_{i,1} = \widehat{B}_i^{-1} P^{-1} Y_1, \quad 1 \leq i \leq 3, \quad (46)$$

$$K_{i,2} = \widehat{B}_i^{-1} P^{-1} Y_2, \quad 1 \leq i \leq 3. \quad (47)$$

Proof. Inspired by [20], the following Lyapunov functions are considered

$$V_{1,1} = \hat{x}(t+1, k+1)^T P \hat{x}(t+1, k+1), \quad (48)$$

$$V_{0,1} = \hat{x}(t, k+1)^T Q \hat{x}(t, k+1), \quad (49)$$

$$V_{1,0} = \hat{x}(t+1, k)^T (P - Q) \hat{x}(t+1, k), \quad (50)$$

where P and Q are symmetric positive matrices to be determined, and $P > Q$.

The state energy increment in both time and batch directions is

$$\Delta V = V_{1,1} - V_{0,1} - V_{1,0}. \quad (51)$$

It follows from (40) and (51) that

$$\Delta V = \xi^T \widehat{\psi} \xi, \quad (52)$$

where

$$\xi = [\hat{x}(t, k+1)^T, \hat{x}(t+1, k)^T]^T, \quad (53)$$

$$\widehat{\psi}_i = \begin{bmatrix} \widehat{A}_{i,1}^T P \widehat{A}_{i,1} - Q & \widehat{A}_{i,1}^T P \widehat{A}_{i,2} \\ \widehat{A}_{i,2}^T P \widehat{A}_{i,1} & \widehat{A}_{i,2}^T P \widehat{A}_{i,2} - P + Q \end{bmatrix}. \quad (54)$$

Therefore, $\Delta V < 0$ guarantees asymptotic stability of closed-loop 2D system in (40).

Applying Schur's complement $\Delta V < 0$ is equivalent to

$$\begin{bmatrix} -P & P\widehat{A}_{i,1} & P\widehat{A}_{i,2} \\ * & -Q & \mathbf{0} \\ * & * & -P + Q \end{bmatrix} < 0. \quad (55)$$

Replace $\widehat{A}_{i,1}$, $\widehat{A}_{i,2}$ with $A_{i,1} + \widehat{B}_i K_{i,1}$, $A_{i,2} + \widehat{B}_i K_{i,2}$, and defining $P\widehat{B}_i K_{i,1} = Y_1$, $P\widehat{B}_i K_{i,2} = Y_2$, LMI constraints in (43) can be obtained. \square

3.4. Controller Parametrization. Theorem 1 is a sufficient and unnecessary condition for system stability, and there are solutions to the LMI Equation (43). The controller with them as parameters stabilizes the system but has different control performance. An efficient combination of linear matrix inequalities and single-objective optimization algorithms was proposed to develop a control law parametrization that guarantees performance [23]. Based on this research, this paper proposes a method of controller parametrization, which combines LMI and multi-objective optimization algorithms.

For the convenience of writing, $K_{i,1}$, $K_{i,2}$ are described as K_1 , K_2 in this section.

In order to measure the control performance of the system, the first function is chosen as

$$f_1(K_1, K_2) = \sum_{k=1}^{\beta} \sum_{t=1}^{\alpha} (y - y_{ref})^2, \quad (56)$$

which is the sum of squares of the output error for all samples in all batches. $f_1(K_1, K_2)$ contains all the system output error information, and the smaller the $f_1(K_1, K_2)$ is, the better the system's dynamic performance and steady-state performance are.

In order to measure the deviation of the output from the reference signal, the second function is chosen as

$$f_2(K_1, K_2) = \sum_{k=1}^{\beta} \max \left\{ |y(t, k) - y_{ref}(t)|_{t \in [1, \alpha]} \right\}. \quad (57)$$

TABLE 2: The plant parameters.

Plant parameter	Abbreviation	Value
The coefficient of the inverter	k_i	5
The weight of the unbalanced mass	m	3.5
The eccentricity of weight from the shaft	E	0.06
The structure coefficient	K	0.882
The equivalent stiffness of springs	k_s	76520
Weight of trough	M	60
The coefficient damping	c	752
The gain of the motor	k_m	0.6
The time-constant of the motor	T	1

TABLE 3: The parameters of the controller.

Controller parameter	Value
$K_{1,1}$	[-1.862, -0.050, 0.150, -0.027, -0.605]
$K_{1,2}$	[0.035, 0.055, 0.020, 0.081, 0.206]
$K_{2,1}$	[-1.959, 0.054, -0.087, 0.052, -0.192]
$K_{2,2}$	[0.034, 0.060, -0.072, -0.124, 0.282]
$K_{3,1}$	[-1.757, 0.005, -0.082, -0.033, 0.015]
$K_{3,2}$	[0.076, 0.052, 0.020, 0.029, 0.291]

After the above discussion, the controller parametrization problem is transformed into the following multi-objective optimization problem:

$$\begin{aligned} \min \quad & [f_1(K_1, K_2), f_2(K_1, K_2)], \\ \text{s.t.} \quad & \psi_i < 0, \quad 1 \leq i \leq 3. \end{aligned} \quad (58)$$

Based on multi-objective simulated annealing [24], the following steps are proposed.

Step 1. Initialize parameters, the initial temperature, T , and the lowest temperature, T_l .

Step 2. Solve the LMI $\psi_i < 0$, apply (46) and (47) to calculate K_1, K_2 , set $K_{1,opt} = K_1, K_{2,opt} = K_2$, simulate (21) and (22) and the nonlinear system with the control law (37), and calculate and set $f_{1,opt} = f_1(K_1, K_2), f_{2,opt} = f_2(K_1, K_2)$.

Step 3. Alter the controller matrices $K_{1,opt}, K_{2,opt}$, obtain the new matrices K_1, K_2 , simulate (21) and (22) and the nonlinear system with the control law (37), and calculate the $f_{1,new} = f_1(K_1, K_2), f_{2,new} = f_2(K_1, K_2)$.

Step 4. If $f_{1,new} < f_{1,opt}$, and $f_{2,new} < f_{2,opt}$, set $K_{1,opt} = K_1, K_{2,opt} = K_2, f_{1,opt} = f_{1,new}, f_{2,opt} = f_{2,new}$. If it does not, calculate $\mu = (1 - \alpha) \cdot (f_{1,new} - f_{1,opt}) / (f_{1,new} + f_{1,opt}) + \alpha \cdot (f_{2,new} - f_{2,opt}) / (f_{2,new} + f_{2,opt})$, and set $K_{1,opt} = K_1, K_{2,opt} = K_2, f_{1,opt} = f_{1,new}, f_{2,opt} = f_{2,new}$ with the probability $P_{accept} = \exp(-(1 - \mu)/T)$.

Step 5. Reduce the temperature T . If $T > T_l$, go to Step 3. If it does not, go to Step 6.

Step 6. Verify $K_{1,opt}, K_{2,opt}$ subject to $\psi_i < 0, 1 \leq i \leq 3$, using $K_{1,opt}, K_{2,opt}$.

4. Simulation

This section gives numerical simulation results, which show that more accurate feed accuracy is obtained after several feeding batches.

The plant parameters are set in Table 2. The discrete state space model is obtained with a sampling period of $T_s = 1$ s. And the weight of material in one batch is set: 20 kg. The duration of a batch is set to 200 s. Then the reference trajectory is obtained

$$y_{ret} = 0.1t, \quad 1 \leq t \leq 200. \quad (59)$$

The controller parameters $K_{i,1}$ and $K_{i,2}$ are obtained by using the controller parameterization method presented in Section 3.4, which is shown as Table 3.

The updating law is obtained by substituting the controller parameters into (37). Then the input voltage is calculated based on (24) and (37), which is the control input applied to the inverter. Then the output response and the process state are obtained in this sampling time. The output responses in all batches are shown in Figure 6.

Figure 6 shows that the output response curve has large fluctuations in the first batch, which means the feeding performance is not good enough. However, the feeding performance is improved. Figure 6 shows that the fluctuation of the output response curve in the latter batch is smaller than the previous.

Figure 7 shows the output response in the first, fourth, and eighth batches, which shows that the errors between the output responses and the reference signal are decreased with the number of batch increasing.

Two performance indicators, the squared error, and the maximum error are presented to evaluate the control performance of the ILC for the weighing and feeding process. The

TABLE 4: Two performance indicators in first 9 batches.

k	1	2	3	4	5	6	7	8	9
Squared error	555	276	123	53	40	35	36	39	34
Maximum error	2.34	2.21	1.56	1.38	1.26	1.17	1.09	1.03	0.98

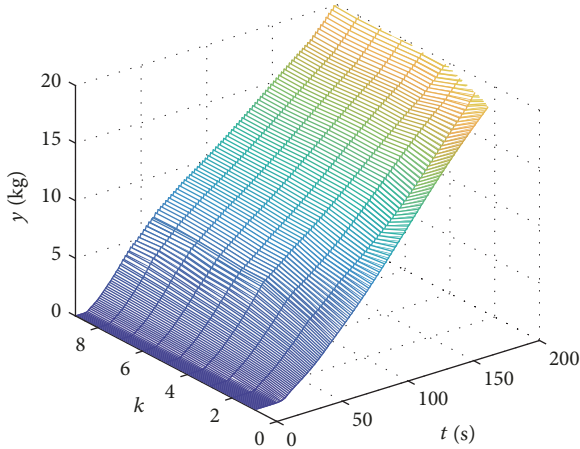
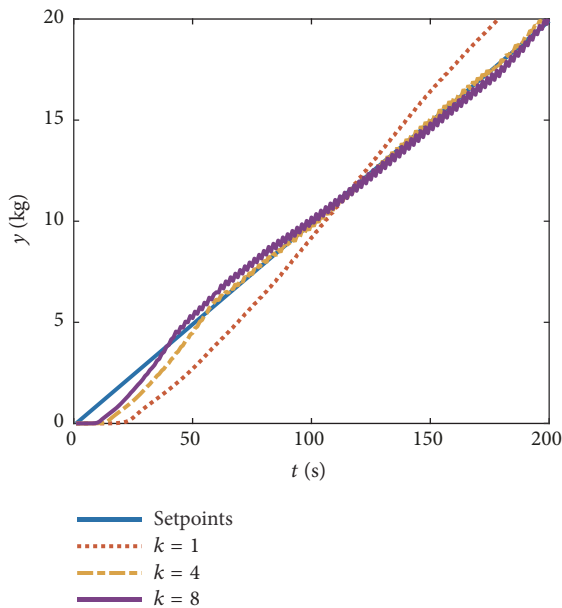


FIGURE 6: Output responses (all batches).

FIGURE 7: Output responses ($k = 1, 4, 8$).

squared error denotes the output error in all sampling time in one batch. The small squared error means good steady-state performance. The maximum error denotes the maximum output error in one batch. The small maximum error means good dynamic state performance. Two performance indicators in the first 9 batches are shown in Table 4. Two values of performance indicators decrease with the number of batch increasing.

Figure 8 shows the change of two performance indicators in the first 9 batches, which demonstrates intuitively that

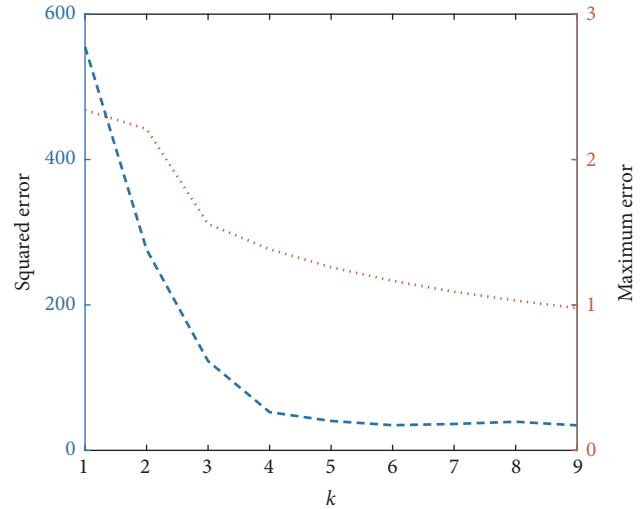


FIGURE 8: Changes in performance indicators.

the two performance indicators decrease with the number of batch increasing. It means that the control performances and the accuracy of feeding are improved with the number of batches increasing, and the accuracy of feeding is acceptable after 3-4 batches.

5. Conclusions

This paper presented an ILC method and a piecewise linearization method for a weighing and feeding process with the nonlinear problem. A piecewise linearization method was presented to establish an approximate linear model. Then an iterative learning controller was designed and the controller parametrization method was given. The simulation result showed that ILC and piecewise linearization effectively solved the control problem of weighing and control process.

Our future work will design a new control method considering the changes in the parameters of the weighing and feeding process model, caused by changes in the properties of the material. And we plan to develop a control system to apply the control method in a real-world weighing and feeding process.

Data Availability

The data used to support the findings of this study are included within the article.

Conflicts of Interest

The authors declare that there are no conflicts of interest regarding the publication of this paper.

Acknowledgments

This work was supported by the Hubei Provincial Natural Science Foundation of China, under Grants 2016CFB480 and 2015CFA010; the National Natural Science Foundation of China, under Grants 61333002 and 61203017; and the 111 Project, under Grant B17040. The first author is an overseas researcher under Postdoctoral Fellowship of Japan Society for the Promotion of Science (JSPS) and his JSPS Fellowship ID is P16799.

References

- [1] S. R. Gopireddy, C. Hildebrandt, and N. A. Urbanetz, "Numerical simulation of powder flow in a pharmaceutical tablet press lab-scale gravity feeder," *Powder Technology*, vol. 302, pp. 309–327, 2016.
- [2] M. A. Parameswaran and S. Ganapathy, "Vibratory conveying-analysis and design: A review," *Mechanism and Machine Theory*, vol. 14, no. 2, pp. 89–97, 1979.
- [3] Ž. V. Despotović, D. Urukalo, M. R. Lečić, and A. Ćosića, "Mathematical modeling of resonant linear vibratory conveyor with electromagnetic excitation: simulations and experimental results," *Applied Mathematical Modelling*, vol. 41, pp. 1–24, 2017.
- [4] P. Czubak, "Analysis of the new solution of the vibratory conveyor," *Archives of Metallurgy and Materials*, vol. 58, no. 4, pp. 1037–1043, 2013.
- [5] M. L. Chandravanshi and A. K. Mukhopadhyay, "Experimental modal analysis of the vibratory feeder and its structural elements," *International Journal of Applied Engineering Research*, vol. 10, no. 13, pp. 33303–33310, 2015.
- [6] M. L. Chandravanshi and A. K. Mukhopadhyay, "Dynamic analysis of vibratory feeder and their effect on feed particle speed on conveying surface," *Measurement*, vol. 101, pp. 145–156, 2017.
- [7] M. L. Chandravanshi and A. K. Mukhopadhyay, "Analysis of variations in vibration behavior of vibratory feeder due to change in stiffness of helical springs using FEM and EMA methods," *Journal of the Brazilian Society of Mechanical Sciences and Engineering*, vol. 39, no. 9, pp. 3343–3362, 2017.
- [8] T. Sato, "Design of a GPC-based PID controller for controlling a weigh feeder," *Control Engineering Practice*, vol. 18, no. 2, pp. 105–113, 2010.
- [9] T. Sato, T. Yamamoto, N. Araki, and Y. Konishi, "Performance-adaptive generalized predictive control-based proportional-integral-derivative control system and its application," *Journal of Dynamic Systems, Measurement, and Control*, vol. 136, no. 6, p. 061003, 2014.
- [10] A. I. Ribić and Ž. V. Despotović, "High-performance feedback control of electromagnetic vibratory feeder," *IEEE Transactions on Industrial Electronics*, vol. 57, no. 9, pp. 3087–3094, 2010.
- [11] Ž. V. Despotović, A. I. Ribić, and V. M. Šinik, "Power current control of a resonant vibratory conveyor having electromagnetic drive," *Journal of Power Electronics*, vol. 12, no. 4, pp. 677–688, 2012.
- [12] F. You and J. An, "Iterative learning control for batch weighing and feeding process," in *Proceedings of the 2018 37th Chinese Control Conference (CCC)*, pp. 2904–2908, Wuhan, China, July 2018.
- [13] X. Hao, L. Liu, Y. Wu, and Q. Sun, "Positive solutions for nonlinear n th-order singular eigenvalue problem with nonlocal conditions," *Nonlinear Analysis, Theory, Methods and Applications*, vol. 73, no. 6, pp. 1653–1662, 2010.
- [14] P. Zhang, L. Liu, and Y. Wu, "Existence and uniqueness of solution to nonlinear boundary value problems with sign-changing Greens function," *Abstract and Applied Analysis*, vol. 2013, no. 1, pp. 1–7, 2013.
- [15] X. L. Lin and Z. Q. Zhao, "Iterative technique for a third-order differential equation with three-point nonlinear boundary value conditions," *Electronic Journal of Qualitative Theory of Differential Equations*, vol. 12, pp. 1–10, 2016.
- [16] Y. Sun, L. Liu, and Y. Wu, "The existence and uniqueness of positive monotone solutions for a class of nonlinear Schrödinger equations on infinite domains," *Journal of Computational and Applied Mathematics*, vol. 321, pp. 478–486, 2017.
- [17] C. Hua, L. Zhang, and X. Guan, "Decentralized output feedback adaptive NN tracking control for time-delay stochastic nonlinear systems with prescribed performance," *IEEE Transactions on Neural Networks and Learning Systems*, vol. 26, no. 11, pp. 2749–2759, 2015.
- [18] C. Hua, L. Zhang, and X. Guan, "Distributed Adaptive Neural Network Output Tracking of Leader-Following High-Order Stochastic Nonlinear Multiagent Systems with Unknown Dead-Zone Input," *IEEE Transactions on Cybernetics*, vol. 47, no. 1, pp. 177–185, 2017.
- [19] M. Uchiyama, "Formulation of high-speed motion pattern of a mechanical arm by trial," *Transactions of the Society of Instrument and Control Engineers*, vol. 14, no. 6, pp. 706–712, 1978.
- [20] T. Liu and F. Gao, "Robust two-dimensional iterative learning control for batch processes with state delay and time-varying uncertainties," *Chemical Engineering Science*, vol. 65, no. 23, pp. 6134–6144, 2010.
- [21] J. Lu, Z. Cao, R. Zhang, and F. Gao, "Nonlinear Monotonically Convergent Iterative Learning Control for Batch Processes," *IEEE Transactions on Industrial Electronics*, vol. 65, no. 7, pp. 5826–5836, 2018.
- [22] J. Emelianova, P. Pakshin, K. Galkowski, and E. Rogers, "Stability of nonlinear discrete repetitive processes with Markovian switching," *Systems and Control Letters*, vol. 75, pp. 108–116, 2015.
- [23] L. Hladowski, K. Galkowski, W. Nowicka, and E. Rogers, "Repetitive process based design and experimental verification of a dynamic iterative learning control law," *Control Engineering Practice*, vol. 46, pp. 157–165, 2016.
- [24] A. Haidine and R. Lehnert, "Multi-Case Multi-Objective Simulated Annealing (MC-MOSA): new approach to adapt simulated annealing to multi-objective optimization," *Engineering and Technology*, vol. 48, no. 12, pp. 705–713, 2008.



Hindawi

Submit your manuscripts at
www.hindawi.com

